IEEE Access
Multidisciplinary ⋮ Rapid Review ⋮ Open Access Journal

Received February 7, 2022, accepted February 28, 2022, date of publication March 8, 2022, date of current version March 22, 2022.

Digital Object Identifier 10.1109/ACCESS.2022.3157914

Broadband and Compact Circularly Polarized MIMO Antenna With Concentric Rings and Oval Slots for 5G Application

JAYSHRI KULKARNI[1], (Senior Member, IEEE), CHOW-YEN-DESMOND SIM[2], (Senior Member, IEEE), RAVI KUMAR GANGWAR[3], (Senior Member, IEEE), AND JAUME ANGUERA[4], (Fellow, IEEE)

[1]Department of Electronics and Telecommunication, Vishwakarma Institute of Information Technology, Pune 411048, India
[2]Department of Electrical Engineering, Feng Chia University, Taichung 40724, Taiwan
[3]Department of Electronics Engineering, Indian Institute of Technology (ISM), Dhanbad 826004, India
[4]Department of Electronics and Telecommunication Engineering, Universitat Ramon Llull, 08022 Barcelona, Spain

Corresponding author: Chow-Yen-Desmond Sim (cysim@fcu.edu.tw)

This work was supported in part by the Ministry of Science and Technology, Taiwan, under Grant MOST-110-2221-E-035-021.

ABSTRACT A broadband and compact size circularly polarized (CP) two-port multiple input multiple output (MIMO) antenna with a footprint of 25 mm × 20 mm is investigated. The designed oval-shaped MIMO antenna employs concentric rings with oval slots (CROS), along with a circular radiator and two open-ended parallel protruded stubs. The CP radiation is achieved by embedding three oval slots, in which two of them are deployed at the left and right side of the concentric rings, whereas the third one is deployed at the top section of the concentric rings. The measured 10-dB impedance bandwidth of the proposed MIMO antenna was 46.30% (3.12–5.00 GHz), and its corresponding 3-dB axial ratio bandwidth (ARBW) was 41.34% (3.30–5.02 GHz). Furthermore, very wide beamwidths of 137°±0.2 and 154°±0.2 were measured in the right-hand circular polarization (RHCP) and left-hand circular polarization (LHCP) radiation patterns, respectively. The minimum achieved isolation between the antenna elements is 18.50 dB without using any additional decoupling structure, and the calculated envelope correlation coefficient (ECC) < 0.03.

INDEX TERMS Antenna, MIMO, 5G, concentric rings, oval slots.

I. INTRODUCTION

Circularly polarized antennas are vital to the wireless communication, satellite communication, wireless local area networks (WLAN), and 5G communication system, as it offers several advantages compared to linearly polarized (LP) antennas [1]–[4], such as preventing multipath interference and fading. To achieve good quality of Service (QoS) and smooth wireless communication, CP antennas has always play a very important role in many wireless communication system. Apart from the above, the CP antennas also helps in overcoming the orientation problem between transmitter and receiver, better mobility due to suppressed multipath interference and better weather penetration as compared to LP antennas [5]. Furthermore, MIMO antennas are desired as they offer larger capacity with higher data rates, low latency, faster mobility, high data throughput, and reliable communication [6], [7]. Therefore, MIMO antenna designs with CP senses have been reported in recent years [8]–[16].

Stacked patch MIMO antennas have the features of wideband/multiband and performance enhancement. Therefore, the work in [8]–[10] has applied the stacked patch technique to the CP MIMO antennas. In [8], corner-truncated square slot and patch configuration are applied to the MIMO antenna to yield CP radiations in 2.45 GHz and 5.8 GHz bands. In [9], the CP is achieved by protruding a stub from the right end of the ground plane, whereas the method applied by [10] is to chamfer the two opposite corners of the ring slot as well as the resonant patch. However, the MIMO antennas in [8] and [10] have exhibited larger dimensions, and the ones in [8] and [9] have used expensive substrates. Notably, applying the stacked patch technique will inevitably increase the overall profile of the designated antenna, which makes it difficult to integrate into a slim wireless device. Even

The associate editor coordinating the review of this manuscript and approving it for publication was Luyu Zhao.

though [11] has introduced a compact CP MIMO antenna designed using two truncated corner square patches with parasitic periodic metallic plates [11], it requires expensive Taconic substrate (same as [8], [9]) that results in higher manufacturing expenses.

To minimize the manufacturing expenses, the works reported in [12]–[16] have introduced MIMO antenna designs using low-cost FR-4 substrate. In [12], an eyebrow-shaped strip is applied to enhance the CP performance of the MIMO antenna, but it has a very large dimension of 85 mm × 73 mm. To reduce the overall MIMO antenna size to 21 mm × 46 mm, split ring resonator was introduced to the MIMO antenna, and good CP radiation is achieved by using offset feeding technique and defective ground structure (DGS) [13]. To further decrease the dimensions to 27 mm × 27 mm, the MIMO antenna design in [14] employs two orthogonally designed T-shaped patches as well as three L-shaped parasitic patches in the ground plane to yield good CP radiation. However, [15] and [16] have shown poor isolation between their respective adjacent antenna elements. To increase the isolation between adjacent antenna elements, [15] has applied the spatial diversity method (adjacent elements separated by a distance of 13.75 mm), and good CP radiation is achieved by applying 90° phased slots at the center of the truncated patch. As for [16], the designed microstrip-fed MIMO antenna is composed of a patch containing two L-shaped radiators along with a wide hexagonal slot radiator on the ground plane, and good 3-dB ARBW of 34.38% and isolation of >17 dB is achieved. In this manuscript, a very low-profile (0.27λ × 0.22λ × 0.01λ) (where λ is calculated at the lowest frequency of 3.30 GHz), oval-shaped CP two-port MIMO antenna for 5G applications is presented. Each CP antenna element is fed by a 50Ω microstrip line and employs CROS, along with a circular radiator, and two open-ended parallel protruded stubs. The oval-shaped slots loaded on the left as well as right side of the concentric rings are for achieving CP radiation, whereas the one that is loaded at the top section is to enhance the ARBW. The proposed CP MIMO antenna can yield RHCP and LHCP radiation when Ant.1 and Ant.2 are excited, respectively. Furthermore, wide 10-dB impedance bandwidth of 46.3% and 3-dB ARBW of 41.34% are also achieved. Notably, the separation distance (center-to-center) of the two antenna elements is only 0.16λ and isolation of up to 18.50 dB can be achieved without applying any additional decoupling structure.

II. GEOMETRY AND DESIGN ANALYSIS OF PROPOSED MIMO ANTENNA

The design layout and fabricated prototype of the proposed CP MIMO/diversity antenna are illustrated in Figures. 1(a) and 1(b), respectively and parameters with their optimized values are articulated in Table 1. The CP MIMO antenna is composed of two identical antenna elements, namely, Ant.1 and Ant.2 (each has a partial ground of size W × L_1), which are printed on an economical FR-4 substrate ($\varepsilon_r = 4.3$, $\delta = 0.025$) of size 25 mm × 20 mm × 1.6 mm. As Ant.1

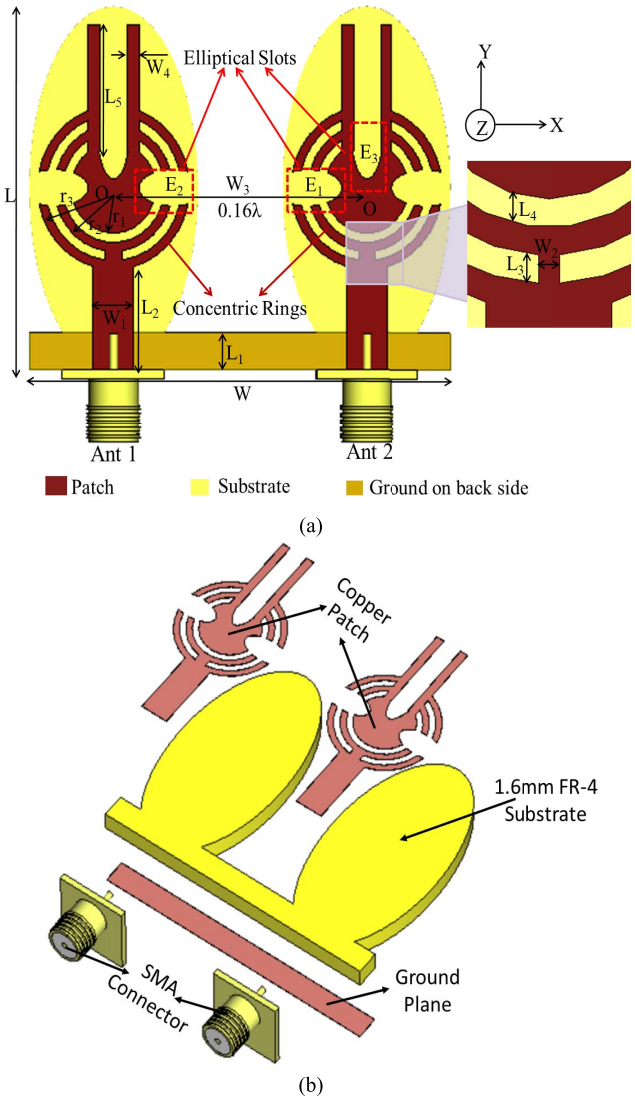

FIGURE 1. Geometry of proposed antenna, (a) Front View (b) Breakdown View.

is the mirror image of Ant.2, they can support polarization diversity, meaning that Ant.1 and Ant.2 radiates RHCP and LHCP waves, respectively. Furthermore, to achieve good isolation, the center-to-center spacing between the two antenna elements (including a partial air gap) is set to be 0.16λ.

In the proposed structure, each antenna element (Ant.1 and Ant.2) is composed of two concentric rings (radius r_2 and r_3) and one circular patch (radius r_1), which shares the same center location 'O'. Here, two elliptical slots having a major and minor axis of 2 mm and 1 mm, respectively, are loaded on the left and right side of the antenna element, and an elliptical slot having a major and minor axis of 3 mm and 1 mm, respectively, is loaded on the top section of the antenna element between two open-ended protruded stubs (each with a dimension of L_5 × W_4). The two antenna elements shared the same partial ground plane of dimension L_1 × W, which is designed on the back of the substrate. The proposed CP

TABLE 1. Dimensions of proposed MIMO antenna.

Parameter	Value (mm)
L	20
L_1	2
L_2	6
L_3	0.5
L_4	0.5
L_5	7
W	25
W_1	2.4
W_2	0.4
W_3	15
W_4	0.7
r_1	2.5
r_{2r}	3.5
r_3	4.5

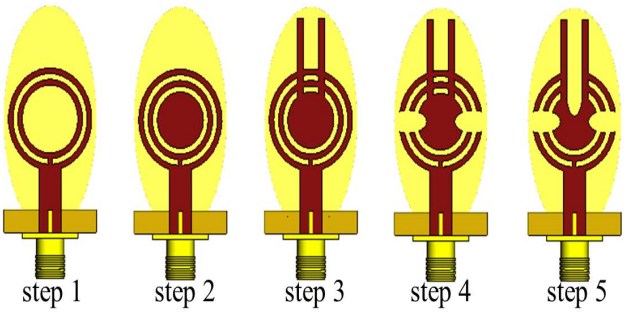

FIGURE 2. Step-wise design of proposed antenna element.

MIMO antenna is simulated (including the SMA connectors) using the 3D EM simulator CST MWS®.

A. STEP-WISE DESIGN OF SINGLE ANTENNA ELEMENT

The step-wise design of the single antenna element is presented in Figure 2. Here, five major steps are analyzed to comprehend the design mechanism, and their corresponding 10-dB impedance bandwidth and 3-dB ARBW are illustrated in Figures 3(a) and 3(b), respectively. As depicted in Figure 2, the proposed antenna element design is stemmed from (Step-1) a circular ring-slot monopole antenna that is loaded by a concentric ring at center location 'O' with radius r_2 and r_3. Notably, this concentric ring is turned into a "split-ring" type by introducing a small shorted section of width 0.5 mm, and resonance at 4.10 GHz is induced with a broad bandwidth of 23.5% (3.60–4.60 GHz), as visualized in Figure 3(a). To further increase the bandwidth, in Step-2, a circular radiator of radius r_1 is loaded into the center ring-slot position, and by further observing Figure 3(a), even though this circular radiator can improve the bandwidth to 38.5% (4.00–5.55 GHz), the resonance mode is shifted towards the higher frequency spectrum (at 4.6 GHz). The broadband behavior in Step-2 is obtained due to the unpunctured and longer path of currents flowing through the circular radiator.

To shift the resonance back to approximately 4 GHz, as well as further improving the operational bandwidth to occupy the complete 5G New Radio (NR) band n77/n78/n79,

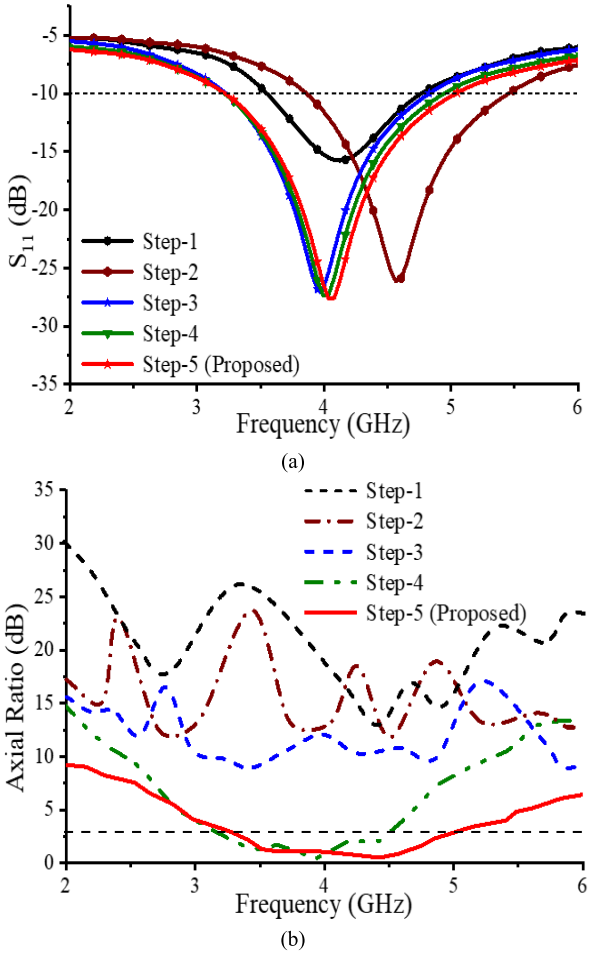

FIGURE 3. (a) S_{11} (dB) (b) Axial Ratio (dB).

in Step-3, two open-ended parallel stubs are protruded from the top section of the antenna element, and a broad bandwidth of (3.18–4.82 GHz) is achieved. However, from Figure 3(b), it is noted that Step-1 to Step-3 can only exhibit LP radiations as their corresponding axial ratio (AR) values are larger than 10 dB. Therefore, to achieve CP radiation across the desired bands of interest, as shown in Figure 2 (Step-4), two elliptical slots are loaded, and the reason for that is to perturb the surface current distribution on the left and right side of the radiator. As illustrated in Figure 3, the antenna in Step-4 has shown a broad 3-dB ARBW of (3.20–4.50 GHz) with desirable 10-dB impedance bandwidth of (3.18–4.90 GHz). Nevertheless, the ARBW of this antenna (Step-4) can only cover the 5G NR band n77/n78 (3.30–4.20 GHz). Therefore, to further increase the ARBW, a top-loaded elliptical slot that acts as a perturbation element is introduced, and the antenna is now denoted as Step-5 (or proposed antenna element) in Figure 2. As shown in Figure 3, the proposed antenna element can yield a wide 3-dB ARBW of 42.42% (3.25–5.00 GHz) with desirable 10-dB impedance bandwidth of 44.50% (3.18–5.00 GHz), and it can fully cover the entire 5G NR band n77/n78/n79 (3.30–5.00 GHz).

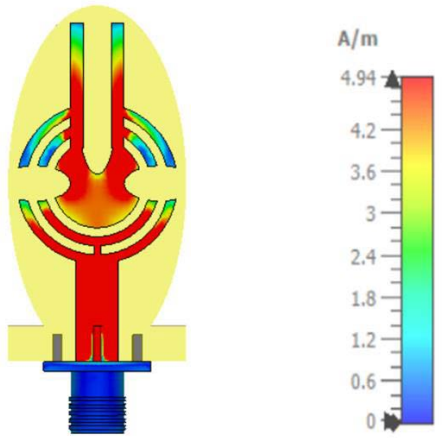

FIGURE 4. Surface current distribution of proposed single antenna element.

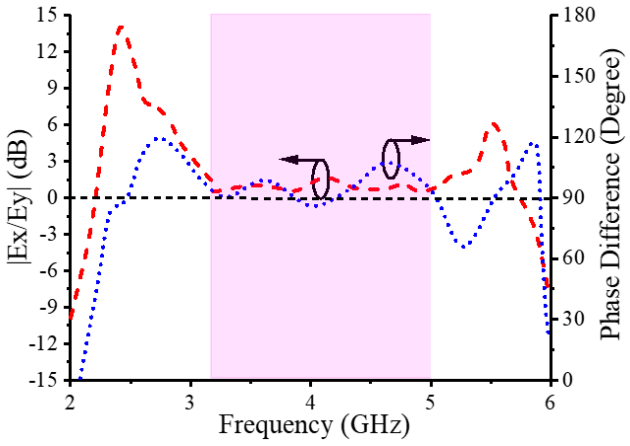

FIGURE 5. Amplitude ratio and phase difference of proposed antenna.

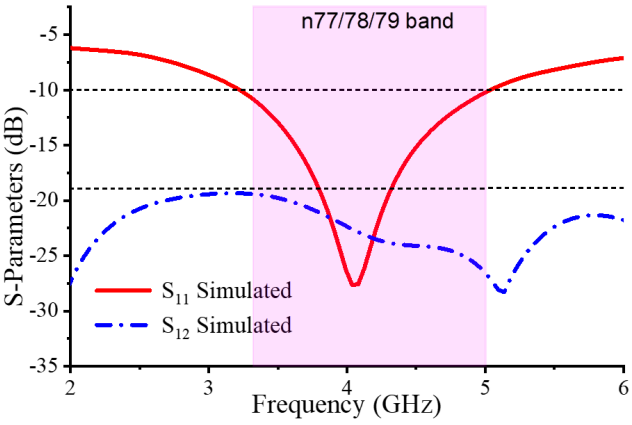

FIGURE 6. Amplitude ratio and phase difference of proposed antenna.

B. SURFACE CURRENT DISTRIBUTION OF PROPOSED ANTENNA

To analyze the working of the proposed antenna, its corresponding simulated surface current (A/m) distribution is analyzed in Figure 4. From Figure 4, it is observed that at 4 GHz, a maximum current is flowing through the circular radiator and at the same time, an equal amount of current flowing through the concentric rings which proves that it helps in generating the resonance as well as widening the bandwidth at 4 GHz. Further equal amount of current is also observed in the two open-ended parallel stub which slightly helps in bandwidth enhancement and tuning the resonance in frequency range of (3.18–5.00 GHz).

C. AMPLITUDE RATIO AND PHASE DIFFERENCE OF PROPOSED ANTENNA

To generate a good CP radiation for an antenna, the horizontal electric field (E_x) and the vertical electric field (E_y) must have an equal amplitude of approximately 1 (or 0 dB) with a phase difference (PD) of 90° throughout the bands of interest. In this regard, to fully comprehend the CP excitation of the proposed antenna element (Step-5), Figure 5 depicts its corresponding calculated amplitude ratio (E_x/E_y) and PD of the two orthogonal electric field components. Here, one can see that the amplitude ratio is closer to 0 dB with PD of near 90° between them. Therefore, the proposed antenna element is a good CP antenna that can be further applied as a MIMO configuration.

D. MIMO ANALYSIS

The simulated S_{11}, S_{22} parameters for the 2-port MIMO antenna geometry shown in Figure 1(a) is obtained by activating Ant.1 and terminating Ant.2 with 50 Ω impedance load and vice versa whereas the transmitting coefficient S_{12}, S_{21} are obtained by activating both the Ant.1 and Ant.2, simultaneously. The curves of S_{22} and S_{21} are not shown for brevity. The simulated S_{11} in Figure 6 illustrates that the bandwidth remains almost the same when the antenna is transformed from single antenna to two antenna elements. The bandwidth obtained for the two-port MIMO antenna array is 44.50% (3.18–5.00 GHz). Similarly, from the transmission coefficient curve S_{12} shown in Figure 6, it is noticed that the isolation between Ant.1 and Ant.2 is larger than 18.5dB throughout the operating band.

To validate the isolation between Ant.1 and Ant.2, the electric field intensity (V/m) distribution on the surface of the two-port MIMO antenna array is illustrated in Figures 7a and 7b, respectively. For analyzing the effect, Ant.1 is excited, while Ant.2 is kept terminated with 50Ω matched impedance load. Under this scenario, from Figure 7a, it is evident that the deployment of antennas at 0.16λ centre-to-centre distance protect the current flowing out from Ant.1 and also suppresses the propagation of surface wave through the ground plane without affecting the impedance matching and radiation performance. Notably, the same is also verified when Ant.2 is excited while the Ant.1 is kept properly terminated with 50Ω matched load.

III. PARAMETRIC ANALYSIS

To validate the geometry of the proposed MIMO antenna, the RF performance of the proposed MIMO antenna in terms of S-parameters is analyzed. The parametric analysis is carried

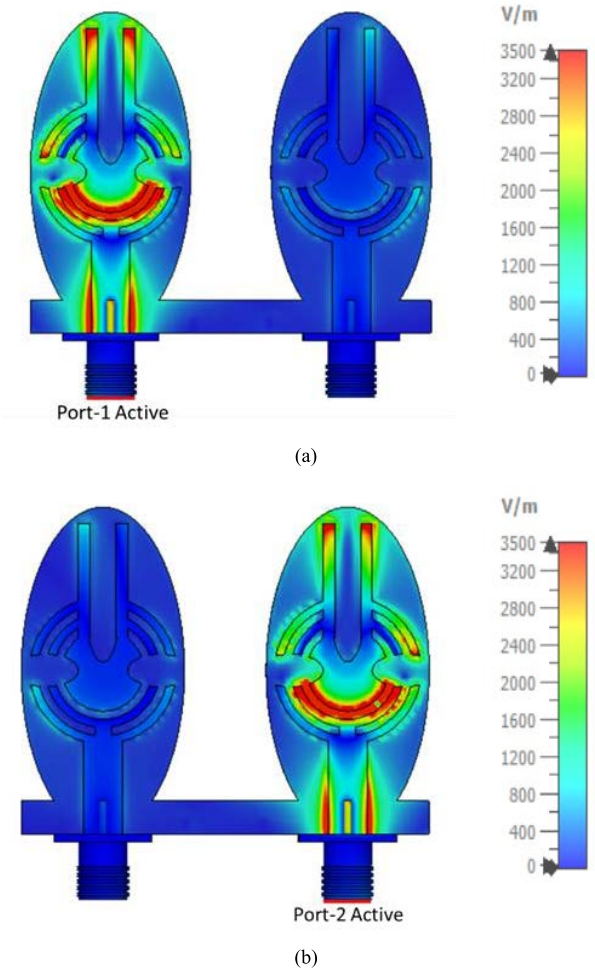

FIGURE 7. Electric Field Intensity of proposed MIMO antenna (a) When Ant.1 is excited (b) When Ant.2 is excited.

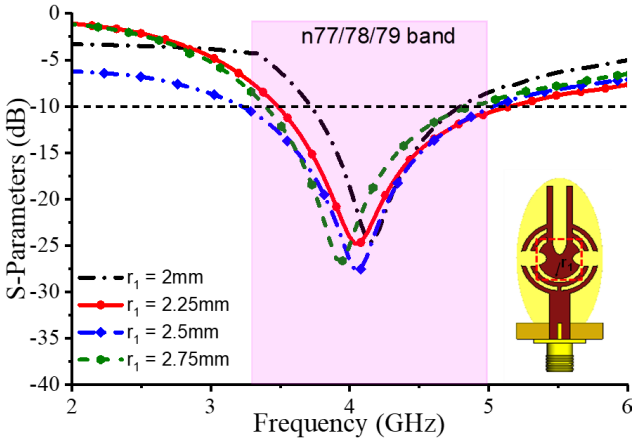

FIGURE 8. Parametric variation of inner circular radius r_1.

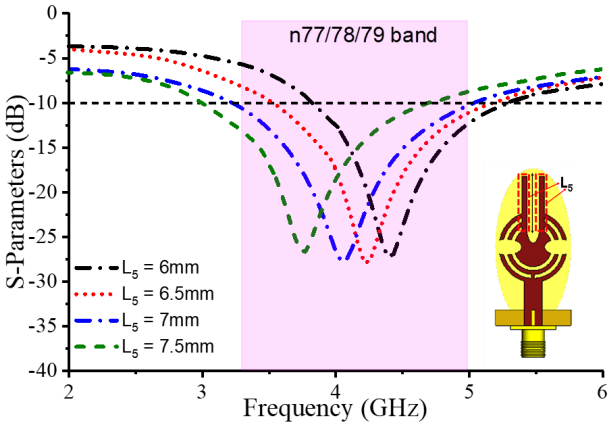

FIGURE 9. Parametric variation of open-ended stubs L_5.

out by varying antenna parameters like radius r_1, open-ended stubs L_5 and centre-to-centre distance w_3 between the antenna elements and keeping all the other parameters constant.

A. EFFECT OF VARYING RADIUS r_1

The inner solid circular radius r_1 is varied from 2mm to 2.75mm as shown in Figure 8. It is analyzed that the -10dB impedance bandwidth increases with increase in radius upto 2.5mm. However, further increase in the radius results in bandwidth reduction (as seen from green line curve) which may be due to the strong coupling between solid radius r_1 and concentric rings when radius is increased beyond 2.5mm. Therefore, the optimum value of radius r_1 is selected as 2.5mm which covers the desired band of operation.

B. EFFECT OF VARYING OPEN-ENDED STUBS L_5

Figure 9 illustrates the variation of open-ended stubs L_5 from 6mm to 7.5mm. It can be observed that increasing the length of the stubs shifts the resonance towards lower frequency whereas small effect is observed on the bandwidth. The value of L_5 is considered as 7mm considering the best RF performance.

C. EFFECT OF VARYING CENTRE TO CENTRE DISTANCE W_3

The effect of varying centre-to centre distance W_3 from 11mm to 17mm on S_{11} and S_{12} is analyzed in Figure 10. It can be observed that the curves for S_{11} remains almost the same for all the values of W_3 whereas better S_{12} curves are observed when the values of W_3 is increased. For W_3 values of 11mm and 13mm the isolation is less than 17dB, whereas for W_3 of 15mm and 17mm the isolation is greater than 18.5dB. Even though the isolation value is greater at 17mm, to restrict the area of the proposed MIMO antenna, the optimum value of 15mm is considered.

IV. RESULTS AND DISCUSSION

The proposed two-port CP MIMO antenna was fabricated, as illustrated in Figure 11, and its typical results such as reflection coefficients (S_{11} and S_{22}), transmission coefficients (S_{12} and S_{21}), AR, two- and three-dimensional radiation patterns, gain, and efficiency were measured and compared with the simulated ones.

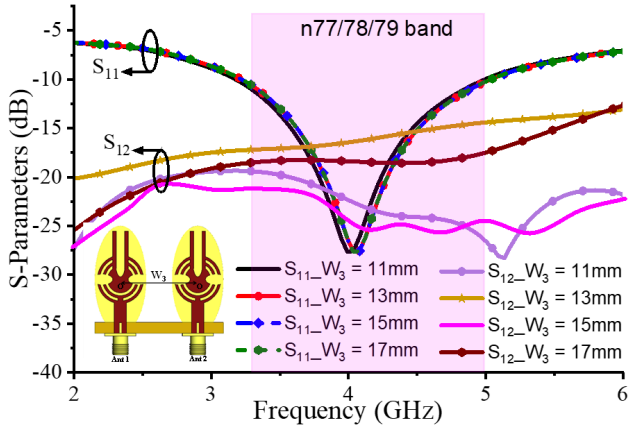

FIGURE 10. Amplitude ratio and phase difference of proposed antenna.

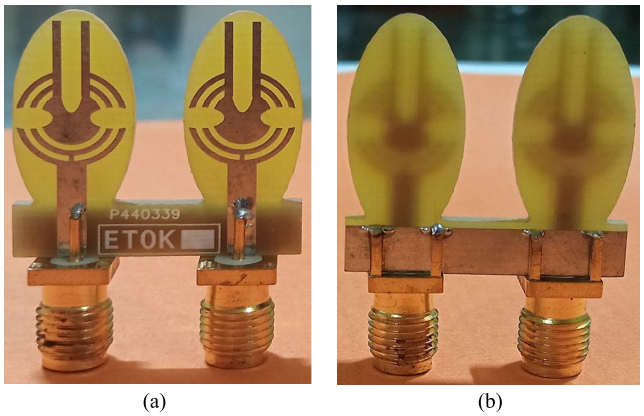

FIGURE 11. Fabricated prototype of proposed MIMO antenna (a) Front View (b) Back View.

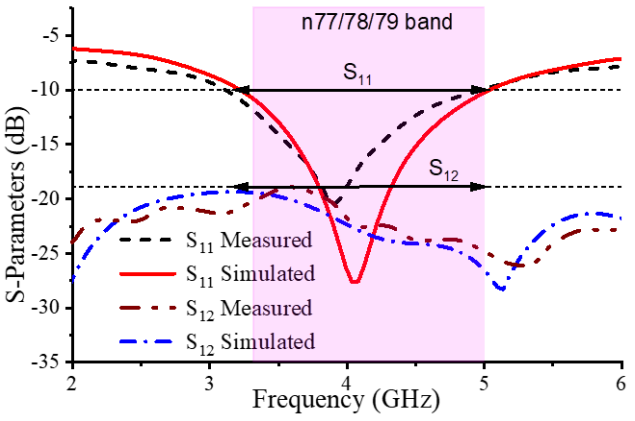

FIGURE 12. Measured and simulated S-parameters of proposed antenna.

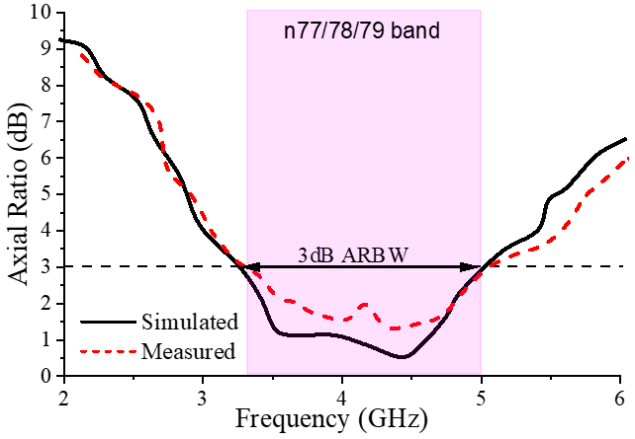

FIGURE 13. Measured and simulated Axial Ratio of proposed antenna.

A. MEASURED AND SIMULATED S-PARAMETERS

The measured and simulated S-parameters (S_{11} and S_{12}) are plotted in Figure 12. While measuring S_{11} and S_{22}, the Ant.1 was activated whereas the Ant. 2 was terminated with 50Ω impedance and vice-versa. While measuring S_{12} and S_{21}, both the Ant.1 and Ant.2 were activated simultaneously. Due to analogy, S_{22} and S_{12} are not shown for brevity. Here, the measured 10-dB impedance bandwidth was approximately 46.30% (3.12 – 5.00 GHz) with a resonance frequency of 4 GHz, and the measured isolation level between antenna elements was larger than 18.5 dB across the bands of interest.

B. MEASURED AND SIMULATED AXIAL RATIO

The measured and simulated AR diagram of the proposed CP MIMO antenna (Ant. 1) is plotted in Figure 13, and a very wide 3-dB ARBW of 41.34% (3.30–5.02 GHz) was measured. By comparing Figure 12 and Figure 13, the measured 3-dB ARBW has overlapped with the impedance bandwidth across the desired bands of interest. The simulated and measured results are well validated with other, and the slight deviation could be due to soldering and fabrication tolerances.

C. VECTOR CURRENT DISTRIBUTION OF PROPOSED ANTENNA

The simulated vector current distributions of the proposed CP MIMO antenna at 4 GHz (with different phases 0°, 90°, 180°, and 270°) are studied in Figures 14(a)-14(d), when both the antenna elements are excited simultaneously. In Figure 14(a), at 0° phase, the maximum current flows in the +y of both the Ant.1 and Ant.2, whereas at 180° phase, the current at both Ant.1 and Ant.2 are flowing in the -y direction, as illustrated in Figure 14(c). At 90° and 270° phases (see Figures 14(b) and 14(d)), the vector current distributions at Ant.1 and Ant.2 are the same in magnitude but flows in opposite phases. Thus, the current vectors are changing with time and rotating in an anti-clockwise manner for Ant.1 (exciting RHCP wave), whereas the current vectors at Ant.2 are rotating in a clockwise direction (exciting LHCP wave).

D. RADIATION CHARACTERISTIC MEASUREMENT SET-UP OF PROPOSED ANTENNA

Figure 15(a) depicts the block diagram whereas Figure 15(b) illustrates the actual set-up of radiation characteristic measurement of proposed MIMO antenna inside anechoic chamber. This set-up is used to measure

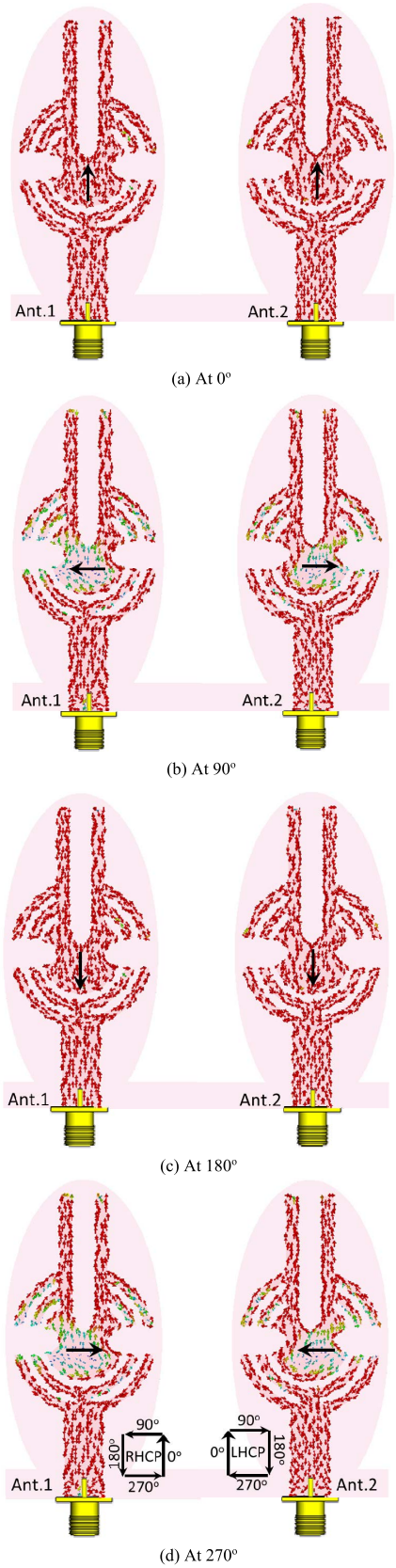

FIGURE 14. Vector current distributions of Ant.1 and Ant.2. (a) 0°, (b) 90°, (c) 180°, (d) 270°.

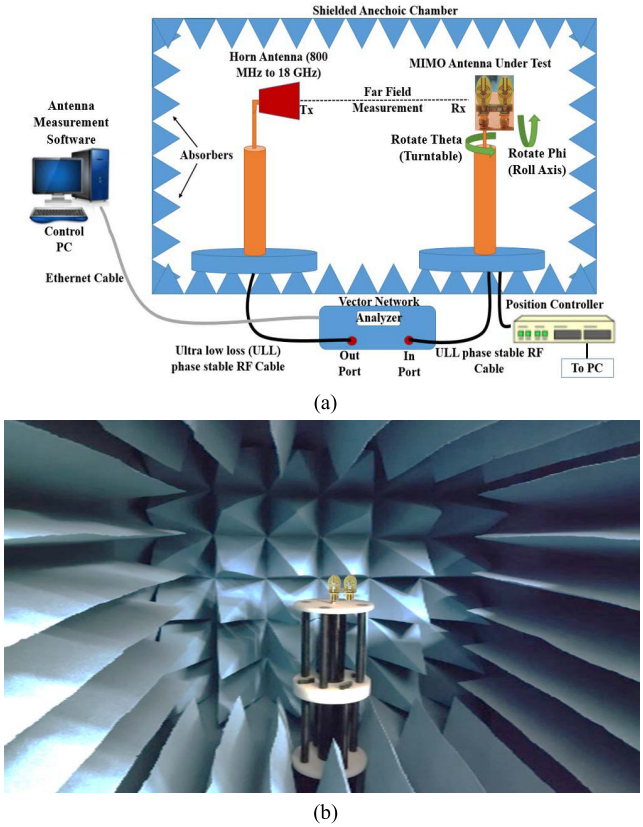

FIGURE 15. Radiation characteristic measurement set-up (a) Block Diagram (b) Actual Set-up in anechoic chamber.

two- and three-dimensional radiation patterns, gain as well as MIMO diversity parameters.

E. TWO-DIMENSIONAL RADIATION PATTERN OF PROPOSED ANTENNA

The radiation patterns of the proposed CP MIMO antenna at 4 GHz (when Ant.1 and Ant.2 are excited individually) are visualized in Figure 16. It is observed that in both the planes ($\phi = 0°$ and $\phi = 90°$), the Ant.1 has demonstrated RHCP operation with a wide 3-dB angular beamwidth of 137°±0.2. In comparison, Ant.2 exhibits LHCP operation in both planes ($\phi = 0°$ and $\phi = 90°$) with a slightly wider 3-dB angular beamwidth of 154°±0.2. This validates the polarization diversity behavior of the proposed two-port CP MIMO antenna.

F. THREE-DIMENSIONAL RADIATION PATTERN OF PROPOSED ANTENNA

The simulated 3D radiation patterns at 4GHz are illustrated in Figure 17. It is visualized that three-dimensional radiation patterns of Ant.1 and Ant.2 are oblique dipole patterns forms mirror image to each other which further validates that the proposed MIMO antenna has good radiation performance.

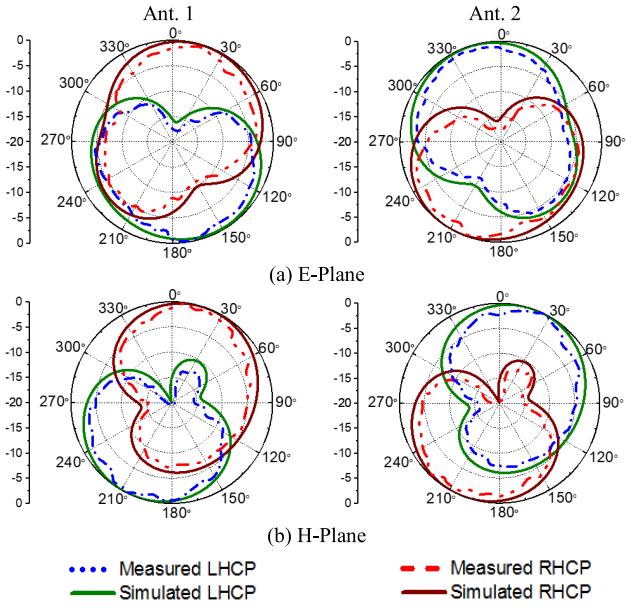

FIGURE 16. Two-Dimensional radiation pattern of proposed antenna (a) E-plane (b) H-plane.

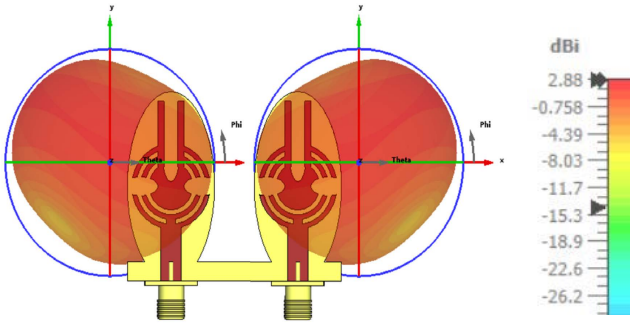

FIGURE 17. Three-Dimensional radiation pattern of proposed antenna.

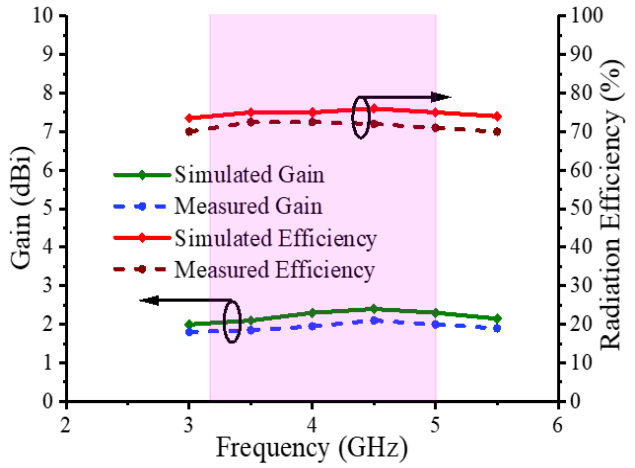

FIGURE 18. Gain and efficiency of proposed antenna.

G. GAIN AND EFFICIENCY OF PROPOSED ANTENNA

The measured and simulated gain and efficiency of the proposed CP MIMO antenna are shown in Figure 18. The measured gain and efficiency were approximately 2.0–2.5 dBi and 70%–75%, respectively, with minimal deviation across 3.12–5.00 GHz.

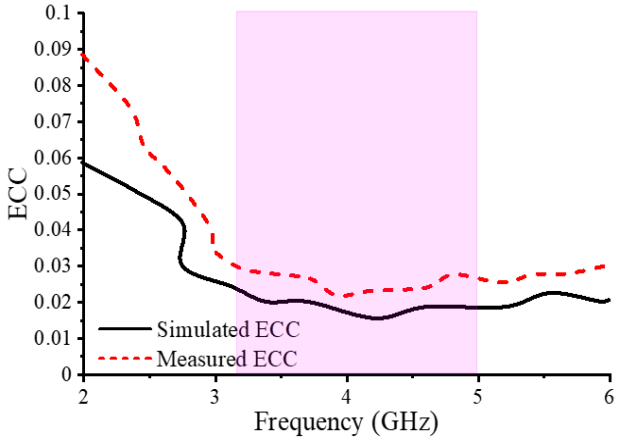

FIGURE 19. ECC of proposed antenna.

V. MIMO DIVERSITY PARAMETERS

A. ECC OF PROPOSED ANTENNA

The ECC is used to verify the performance of the proposed CP MIMO antenna for diversity applications. It is calculated from far-field patterns using formula mentioned in [17]. As shown in Figure 19, the ECC values are less than 0.03 across the operating bands, which confirms that the designed CP MIMO antenna has good isolation and offer best performance under the influence of multipath fading environments.

B. MEG OF PROPOSED ANTENNA

MEG is a crucial parameter for the diversity performance analysis of any MIMO system. Therefore, the MEG is defined as the ratio of power received by MIMO antenna to the power received by isotropic antenna. In MIMO system, the MEG is calculated using equations (1-3).

$$\text{MEG-i} = 0.5\left[1 - \sum_{j=1}^{M} |S_{ij}|^2\right] \tag{1}$$

where, M is the number of antenna elements and 'i' is the port number. By expanding the above equation, the MEG-1 for port-1 is found as:

$$\text{MEG-1} = 0.5\left[1 - |S_{11}|^2 = |S_{12}|^2\right] \tag{2}$$

and the MEG-2 for port-2 is found as:

$$\text{MEG-2} = 0.5\left[1 - |S_{21}|^2 = |S_{22}|^2\right] \tag{3}$$

For better diversity metrics, the MEG-1 and MEG-2 values as per industry standard, should be $-3 \leq \text{MEG (dB)} \leq -12$, whereas the ratio of MEG-1/MEG-2 should be approximately equal to 1. From Table 2, it is validated that the MEG values as well as the ratio are within the well-defined limit.

TABLE 2. MEG values of proposed MIMO antenna.

Frequency (GHz)	MEG-1	MEG-2	MEG-1/MEG-2
3.5	-3.82	-3.83	0.997
4	-3.82	-3.85	0.992
4.5	-3.83	-3.84	0.997
5	-3.85	-3.82	1.007

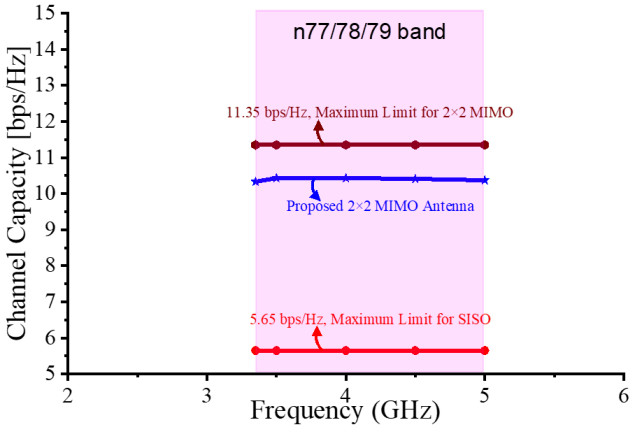

FIGURE 20. Channel capacity of proposed antenna.

C. CHANNEL CAPACITY OF PROPOSED ANTENNA

The ergodic channel capacity of the proposed MIMO antenna across the operating bands is analysed in Figure 20 using the following equation (4).

$$C = k\{log_2 det[I + \eta \frac{SNR}{k} HH^*] \quad (4)$$

where in equation (4), k *is* the number of antenna elements, SNR defines the mean signal to noise ratio, [I] denotes an identity matrix, η indicates the efficiency, $[H]$ is the normalized channel matrix considered as frequency independent over the operating bands, and H^* denotes the transpose conjugate matrix of H.

The MIMO systems channel model should be selected first while calculating the channel capacity and the model for ray tracing or the associated statistical model is mostly used. So, based on the correlation matrix method, the 4-port MIMO antenna's channel capacity is calculated. The calculated channel capacity of the proposed array is indicated in Table 3 as well as in Figure 20, which is between 10 and 10.5 bps/Hz by considering simulated efficiencies (η) and averaging 10,000 Rayleigh fading realizations with 20dB SNR in the identically and independently distributed propagation condition [18]. For maximum channel capacity, all channels have no correlation, and fading matrix [H][H*] is converted into an identity matrix.

The channel capacity of the proposed two-port MIMO antenna is above 10.3bps/Hz throughout the operating band, which is about 1.82 times greater than the maximum limit of an ideal Single antenna (about 5.65 bps/Hz). Compared with the maximum limit for an ideal two-port MIMO antenna, the proposed MIMO antenna have exhibited good channel capacities.

TABLE 3. Channel capacities values of proposed MIMO antenna.

Frequency (GHz)	Channel Capacity (bps/Hz)
3.5	10.43
4	10.43
4.5	10.41
5	10.37

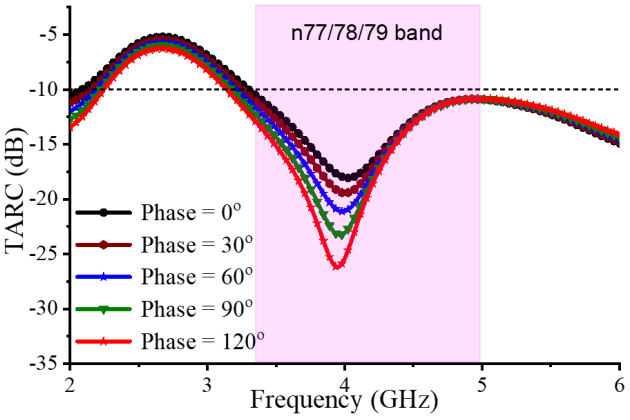

FIGURE 21. TARC of proposed antenna.

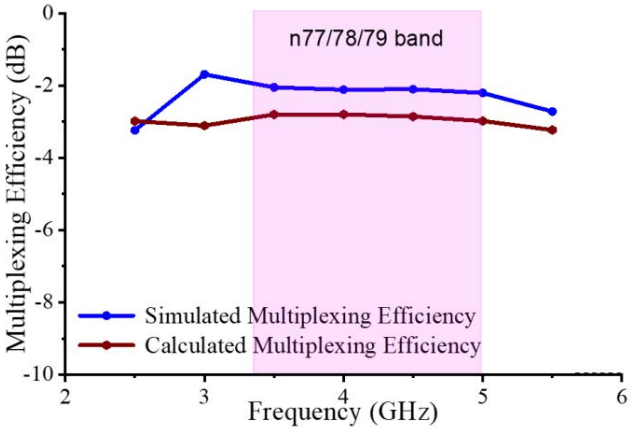

FIGURE 22. Simulated and calculated multiplexing efficiency of proposed antenna.

D. TARC OF PROPOSED ANTENNA

The Total Active Reflection Coefficient (TARC) between Ant. 1 and Ant. 2 is calculated using the below Equation (5).

$$\Gamma = \frac{\sqrt{(|S_{ij} + S_{ij}e^{j\theta}|^2) + (|S_{ji} + S_{jj}e^{j\theta}|^2)}}{\sqrt{2}} \quad (5)$$

where θ is the input phase angle varied from 0^0 to 120^0 at an interval of 30^0, S_{ii} and S_{jj} are the reflection coefficients of the port i and port j, respectively. Figure 21 depicts the TARC values for antenna elements, where it is visualized that under the variation of phase angle, the performances of the proposed MIMO antenna remain unaltered in the scattering environment.

E. MULTIPLEXING EFFICIENCY OF PROPOSED ANTENNA

Multiplexing efficiency is the signal-to-noise ratio between imperfect MIMO antenna and the ideal antenna and can be

TABLE 4. Comparison of proposed antenna with recent CP MIMO antennas.

Ref.	Size (mm^2)	Bands (GHz)	ARBW (GHz)	Isol. (dB)	Gain (dBi)	ECC
[7]	119×119	2.4–2.48 5.72–5.87	2.41–2.49 5.62–5.96	30	10	< 0.03
[8]	13.7×36.2	5.20–6.30	5.20–6.30	20	6	< 0.004
[9]	96×96	2.36–2.53	2.30–2.50	25	8	< 0.004
[10]	45×32	5.10–5.85	5.10–5.85	20	5	< 0.05
[11]	85×73	3.50–8.20	4.60–7.60	20	10	< 0.4
[12]	21×46	3.18–3.90 4.94–7.73	6.65–6.92	15	3.4	< 0.1
[13]	27×27	2.20–6.80	4.00–4.47 5.10–5.22	14	5.5	-
[14]	27.6×97	5.49–6.02	5.74–5.83	34	5.34	< 0.1
[15]	25×25	3.00–11.0	4.00–5.50	17	4.9	< 0.15
This Work	25×20	3.12–5.00	3.30–5.02	18	2.5	< 0.01

calculated using below formula (6) [19]:

$$\eta_{mux} = \sqrt{\eta_i \eta_j (1 - |\rho_c|^2)} \tag{6}$$

As illustrated in Figure 22, both the simulated as well as calculated multiplexing efficiency is higher than -3dB throughout the operating band which satisfy the requirements of MIMO wireless communication systems.

VI. PERFORMANCE COMPARISON OF PROPOSED ANTENNA WITH EXISTING STATE OF ART

The performance comparison of designed CP MIMO antenna with recent literature is compared in Table 4. From the below table it can be noted that the proposed MIMO antenna has smallest dimension, as well as covers the complete 5G sub-6GHz band with overlapping 3dB ARBW in the desired band as compared to the all the reported CP MIMO Antennas.

VII. CONCLUSION

A compact size dual CP MIMO antenna with broad ARBW has been successfully investigated. The proposed CP MIMO geometry is composed of two antenna elements arranged in a mirrored pattern to each other, in which Ant.1 and Ant.2 can induce RHCP and LHCP radiation, respectively. The proposed CP MIMO antenna has demonstrated a broad impedance bandwidth of 46.30% (3.12–5.00 GHz) with wide ARBW of 41.34% (3.30–5.02 GHz). Furthermore, peak gain of up to 2.5 dBi and efficiency of >70% were measured. Therefore, the proposed dual CP MIMO antenna is a good candidate for 5G NR band n77/n78/n79 communication applications.

REFERENCES

[1] S. Gao, Q. Luo, and F. Zhu, *Circularly Polarized Antennas*. West Sussex, U.K.: Wiley, 2014, pp. 1–26.
[2] U. Banerjee, A. Karmakar, and A. Saha, "A review on circularly polarized antennas, trends and advances," *Int. J. Microw. Wireless Technol.*, vol. 12, no. 9, pp. 922–943, 2020.
[3] S. Sharma and C. C. Tripathi, "A comprehensive study on circularly polarized antenna," in *Proc. 2nd Int. Innov. Appl. Comput. Intell. Power, Energy Controls Impact Humanity (CIPECH)*, Nov. 2016, pp. 234–239.
[4] M. Samsuzzaman and M. Islam, "Circularly polarized broadband printed antenna for wireless applications," *Sensors*, vol. 18, no. 12, p. 4261, Dec. 2018.
[5] N. Ojaroudi Parchin, H. J. Basherlou, and R. A. Abd-Alhameed, "Dual circularly polarized crescent-shaped slot antenna for 5G front-end systems," *Prog. Electromagn. Res. Lett.*, vol. 91, pp. 41–48, 2020.
[6] J. Kulkarni, A. Desai, and C. Y. D. Sim, "Wideband four-port MIMO antenna array with high isolation for future wireless systems," *AEU-Int. J. Electron. Commun.*, vol. 128, Jan. 2021, Art. no. 153507.
[7] J. Kulkarni, A. Desai, and C. Y. D. Sim, "Two port CPW-fed MIMO antenna with wide bandwidth and high isolation for future wireless applications," *Int. J. RF Microw. Comput.-Aided Eng.*, vol. 31, no. 8, Aug. 2021, Art. no. e22700.
[8] E. Zhang, A. Michel, P. Nepa, and J. Qiu, "Compact dual-band circularly polarized stacked patch antenna for microwave-radio-frequency identification multiple-input-multiple-output application," *Int. J. Antennas Propag.*, vol. 2021, pp. 1–13, May 2021.
[9] U. Ullah, I. B. Mabrouk, and S. Koziel, "Enhanced-performance circularly polarized MIMO antenna with polarization/pattern diversity," *IEEE Access*, vol. 8, pp. 11887–11895, 2020.
[10] E. Zhang, A. Michel, M. R. Pino, P. Nepa, and J. Qiu, "A dual circularly polarized patch antenna with high isolation for MIMO WLAN applications," *IEEE Access*, vol. 8, pp. 117833–117840, 2020.
[11] H. H. Tran, N. Hussain, and T. T. Le, "Low-profile wideband circularly polarized MIMO antenna with polarization diversity for WLAN applications," *AEU-Int. J. Electron. Commun.*, vol. 108, pp. 172–180, Aug. 2019.
[12] M. Jalali, M. Naser-Moghadasi, and R. A. Sadeghzadeh, "Dual circularly polarized multilayer MIMO antenna array with an enhanced SR-feeding network for C-band application," *Int. J. Microw. Wireless Technol.*, vol. 9, no. 8, pp. 1741–1748, Oct. 2017.
[13] M. Ameen, O. Ahmad, and R. Chaudhary, "Single split-ring resonator loaded self-decoupled dual-polarized MIMO antenna for mid-band 5G and C-band applications," *AEU-Int. J. Electron. Commun.*, vol. 124, Sep. 2020, Art. no. 153336.
[14] X. Xiong, B. W.-K. Ling, H. Zhang, and G. Zhang, "Coplanar waveguide fed multiple input multiple output antenna with higher isolation and multi-sense circular polarization," *J. Electromagn. Waves Appl.*, vol. 32, no. 6, pp. 685–694, Apr. 2018.
[15] L. Malviya, R. K. Panigrahi, and M. V. Kartikeyan, "Circularly polarized 2×2 MIMO antenna for WLAN applications," *Prog. Electromagn. Res. C*, vol. 66, pp. 97–107, 2016.
[16] S. Saxena, B. K. Kanaujia, S. Dwari, S. Kumar, and R. Tiwari, "A compact dual-polarized MIMO antenna with distinct diversity performance for UWB applications," *IEEE Antennas Wireless Propag. Lett.*, vol. 16, pp. 3096–3099, 2017.
[17] S. Kumar, G. H. Lee, D. H. Kim, H. C. Choi, and K. W. Kim, "Dual circularly polarized planar four-port MIMO antenna with wide axial-ratio bandwidth," *Sensors*, vol. 20, no. 19, p. 5610, Sep. 2020.
[18] J. Kulkarni, A. Desai, and C. Y. D. Sim, "Two port CPW-fed MIMO antenna with wide bandwidth and high isolation for future wireless applications," *Int. J. RF Microw. Comput.-Aided Eng.*, vol. 31, no. 8, Aug. 2021, Art. no. e22700.
[19] W. Yin, S. Chen, J. Chang, C. Li, and S. K. Khamas, "CPW fed compact UWB 4-element MIMO antenna with high isolation," *Sensors*, vol. 21, no. 8, p. 2688, Apr. 2021.

JAYSHRI KULKARNI (Senior Member, IEEE) received the B.E. degree in electronics and telecommunication engineering from the Shivaji University, Maharashtra, India, in 2005, the M.E. degree in microwave engineering from PICT College, Pune, Maharashtra, in 2011, and the Ph.D. degree in electronics and communication engineering from Anna University, Chennai, India, in 2020.

From 2006 to 2009, she was a Lecturer with the Genba Sopanrao Moze College of Engineering, Pune. Since 2010, she has been working as an Assistant Professor with the Department of Electronics and Telecommunication Engineering, Vishwakarma Institute of Information Technology, Pune. She has authored more than ten books and more than 30 research papers in reputed journals and conferences. Her research interests include antennas, microwave engineering, wireless communication, and wireless sensor networks.

Dr. Kulkarni awards include Desmond Sim Award for best antenna design paper at IEEE InCAP 2019, India; the Outstanding Oral Presentation Award at ICRAMET-2020, Indonesia; and the Best Paper of the Session Award at IEEE ESCI-2021, Pune.

CHOW-YEN-DESMOND SIM (Senior Member, IEEE) was born in Singapore, in 1971. He received the B.Sc. degree from the Engineering Department, University of Leicester, U.K., in 1998, and the Ph.D. degree from the Radio System Group, Engineering Department, University of Leicester, in 2003. From 2003 to 2007, he was an Assistant Professor with the Department of Computer and Communication Engineering, Chienkuo Technology University, Changhua, Taiwan. In 2007, he joined the Department of Electrical Engineering, Feng Chia University (FCU), Taichung, Taiwan, as an Associate Professor, where he became a Full Professor in 2012 and as a Distinguish Professor in 2017. He has served as the Executive Officer of the Master's Program with the College of Information and Electrical Engineering (Industrial Research and Development), the Director of Intelligent IoT Industrial Ph.D. Program, from August 2015 to July 2018. He co-founded the Antennas and Microwave Circuits Innovation Research Center in Feng Chia University and served as the Director, from 2016 to 2019. He has served as the Head of the Department of Electrical Engineering, Feng Chia University, from August 2018 to July 2021. He has authored or coauthored over 170 SCI papers. His current research interests include antenna design, VHF/UHF tropospheric propagation, and RFID applications. He is a fellow of the Institute of Engineering and Technology (FIET), a Senior Member of the IEEE Antennas and Propagation Society, and a Life Member of the IAET. He served as a TPC Member of the APMC 2012, the APCAP 2015, IMWS-Bio 2015, CSQRWC 2016, ICCEM 2017, APCAP 2018, CIAP 2018, and ISAP 2019. He has also served as the TPC Sub-Committee Chair (Antenna) of the ISAP 2014, PIERS 2017, and PIERS 2019. He was invited as the Workshop/Tutorial Speaker at APEMC 2015, iAIM 2017, and InCAP 2018, and an Invited Speaker of TDAT 2015, iWAT 2018, APCAP 2018, ISAP 2019, and InCAP 2019. He was the Keynote Speaker of SOLI 2018. He has served as the Advisory Committee of InCAP 2018/2019, and has also served as the TPC Chair of the APCAP 2016 and iWEM 2019. He was the General Co-Chair of ISAP 2021. He has served as the Chapter Chair of the IEEE AP-Society, Taipei Chapter (from January 2016 to December 2017), and he is the founding Chapter Chair of the IEEE Council of RFID, Taipei Chapter (since October 2017). He is now serving as an Associate Editor of IEEE Antennas and Wireless Propagation Letters, IEEE Access, IEEE Journal of Radio Frequency Identification, and *International Journal of RF and Microwave Computer-Aided Engineering* (Wiley). Since October 2016, he has been serving as the Technical Consultant for SAG (Securitag Assembly Group), which is one of the largest RFID tag manufacturers in Taiwan. He is also serving as a Consultant of Avary (the largest PCB manufacturer in mainland China), since August 2018. He was a recipient of the IEEE Antennas and Propagation Society Outstanding Reviewer Award (IEEE Transactions on Antennas and Propagation) for six consecutive years, from 2014 to 2019. He has also received the Outstanding Associate Editor Award from the IEEE Antennas Wireless and Propagation Letters, in July 2018.

RAVI KUMAR GANGWAR (Senior Member, IEEE) received the B.Tech. degree in electronics and communication engineering from Uttar Pradesh Technical University, Lucknow, and the Ph.D. degree in electronics engineering from the Indian Institute of Technology (Banaras Hindu University) Varanasi, Varanasi, India, in 2006 and 2011, respectively. He is currently an Associate Professor with the Department of Electronics Engineering and the Associate Dean (Sponsored Research and Industrial Consultancy) of the Indian Institute of Technology (Indian School of Mines) Dhanbad, India. He has guided/guiding 15 Ph.D. and 19 M.Tech. students. He has completed/ongoing eight research and development projects (≈2 Crores rupees) related dielectric resonator antennas and their applications from various funding agencies, like DRDO, SERB-DST, and ISRO. He has authored or coauthored over 100 research articles in reputed international journals and 80 papers in conference proceedings. His research interests include dielectric resonator antennas, microstrip antennas, and bio-electromagnetics. He is a Senior Member of the Antenna and Propagation Society, the Institute of Electrical and Electronics Engineers (IEEE), USA; a member of the Institution of Engineering and Technology (IET), U.K.; a Life Member of the Institution of Engineers (IE), India; and a fellow of the Institution of Electronics and Telecommunication Engineers (IETE), India. He is also a member of the IETE Executive Council and a Joint Regional Secretary at the Ranchi Centre. He is an External Expert of the peer-review committee of project related to chaff application of the Defence Laboratory Jodhpur, DRDO. He was a recipient of the INSA Visiting Scientist Fellowship and the IETE Smt. Ranjana Paul Memorial Award, for the year 2020. He is an Associate Editor of IEEE Access and *IET Circuits, Devices & Systems* journal. He is a Reviewer of IEEE Transactions on Antennas and Propagation, IEEE Antenna and Propagation Letters, *IEEE Antenna and Propagation Magazine*, *IET Microwave, Antenna & Propagation*, *IET Electronics Letters*, *Microwave and Optical Technology Letters*, and *Scientific Report*.

JAUME ANGUERA (Fellow, IEEE) was born in Vinaròs, Spain, in 1972. He received the Technical Engineering degree (three years degree) in electronic systems and the Engineering degree (five years degree) in electronic engineering from Universitat Ramon LLull (URL), Barcelona, Spain, in 1994 and 1998, respectively, and the Telecommunication Engineering degree (five years degree) and the Ph.D. degree in telecommunications from the Polytechnic University of Catalonia (UPC), Barcelona, in 1998 and 2003, respectively.

From 1997 to 1999, he joined the Electromagnetic and Photonic Engineering Group, Signal Theory and Communications Department, UPC, as a Researcher in microstrip fractal-shaped antennas. In 1999, he was a Researcher at Sistemas Radiantes, Madrid, Spain, where he was involved in designing a dual-band dual-polarized fractal-inspired microstrip patch arrays for mobile communications. In 1999, he became an Assistant Professor at the Department of Electronics and Telecommunications, URL, and an Associate Professor, in 2016, where he is currently teaching antenna theory. He is also a Co-Founder and the CTO at Ignion, Barcelona. Since 2001, he has led research projects in the antenna field for wireless applications in a frame of Industry-University collaboration with Ignion and the Department of Electronics and Telecommunications, URL. Several of his supervised students have been awarded the Best Bachelor's and Master's Thesis Award by the Spanish Ministry and other Spanish Institutions. From 1999 to 2017, he was with Fractus (founder partner), Barcelona, where he was a Research and Development Manager and has developed various cutting-edge antenna technologies. At Fractus, he led projects on antennas for base station systems antennas for automotive. From 2003 to 2006, he was also assigned to Fractus, South Korea, to head up the research team. One of his main tasks was to provide training, education, and development of the team's core competency and provide a research and development vision to address the rapidly growing mobile device market. Under his leadership, the company had secured major contracts with companies, such as Samsung, LG, and Bellwave. Since 2017, he has been with Ignion with the role of CTO. He leads the company's research and development activity to create new products, envisage new technologies, technical evangelism, foster synergies with partners, and provide technology strategy to scale the company's business. He holds more than 150 granted invention patents (USA, Asia, and Europe) in the antenna field, many of which have been licensed to antenna companies. Among his most outstanding contributions is that of inventor of Antenna Booster Technology, a technology that fostered the creation of Ignion. The wireless industry has adopted many of these products worldwide to allow wireless connectivity to IoT devices through a miniature component called an antenna booster that is ten times smaller than conventional antennas. He published a book about *Korean Experiences* (in 2015). He is the author of more than 250 journals, international and national conference papers (H-index=51 with more than 8000 citations based on Google Scholar). He has taught more than 40 antenna courses around the world (USA, China, Korea, India, U.K., France, Poland, Czech Republic, Tunisia, Perú, Brazil, Canada, and Spain). He has directed more than 150 bachelor, master, and Ph.D. theses.

He has authored seven books. He has participated in over 20 national/international projects and research grants valued at over €8 million, in which he was the principal researcher in many of them. His current research interests include antenna boosters, multiband and small antennas, broadband matching networks, diversity antenna systems/MIMO, electromagnetic dosimetry, genetically optimized antennas, and antennas for wireless handset devices. He was a member of the fractal team that in 1998 received the European Information Technology Grand Prize for the Applied Science and Engineering for the fractal-shaped antenna application to cellular telephony and the 2003 Finalist to the Best Doctoral Thesis on UMTS (Fractal and Broadband Techniques on Miniature, Multi-frequency, and High-Directivity Microstrip Patch Antennas), prize promoted by ''Technology plan of UMTS promotion'' given by Telefónica Móviles España). New faces of Engineering 2004 (promoted by IEEE and IEEE Foundation). In 2004, he won the Best Doctoral Thesis (Ph.D.) Award in ''network and broadband services'' (XXIV Prize Edition ''Ingenieros de Telecomunicación'') organized by the Colegio Oficial de Ingenieros de Telecomunicación (COIT) and the Company ONO (National Price). In 2011, he received the Alé Vinarossenc recognition by Fundació Caixa Vinarós. In 2014, together with four other Fractus inventors, he received the ''2014 Finalist to European Patent Award.'' He is a reviewer of several IEEE journals and others. He is an Associate Editor of IEEE Open Journal on Antennas and Propagation and Electronics Letters. His biography is listed in Who's Who in the World, Who's Who in Science and Engineering, Who's Who in Emerging Leaders, and International Biographical Center, Cambridge-England (IBC). He is an IEEE Antennas and Propagation Distinguished Lecturer and the Vice-Chair of the working group ''Software and Modeling'' at EurAAP. His detailed information can be found at: http://users.salleurl.edu/ jaume.anguera/.